The unusual optical afterglow of the gamma-ray burst GRB 021004: Color changes and short-time-scale variability[1]

D. Bersier[2], K. Z. Stanek[2], J. Winn[2,3], T. Grav[2,4], M. J. Holman[2], T. Matheson[2], B. Mochejska[2,5] D. Steeghs[2], A. R. Walker[6], P. M. Garnavich[7], J. Quinn[7], S. Jha[8], H. Calitz[9], P. Meintjes[9]

ABSTRACT

We report $UBVRI$ observations of the optical afterglow of the gamma-ray burst GRB 021004. We observed significant ($\sim 10-20\%$) deviations from a power law decay on several time scales, ranging from a few hours down to 20-30 minutes. We also observed a significant color change starting ~ 1.5 days after the burst, confirming and extending the spectroscopic results already reported by Matheson et al. (2002). We discuss these results in the context of several models that have recently been proposed to account for the anomalous photometric behavior of this event.

Subject headings: gamma-ray: bursts

1. Introduction

The gamma ray burst GRB 021004 was discovered by HETE at 12:06 UT on 4 October 2002 (Shirasaki et al. 2002). Observations beginning less than 10 minutes after the burst

[1]Based on data from the FLWO 1.2m telescope, the Magellan 6.5m Landon Clay telescope, the CTIO Blanco 4m telescope, the 1.8m Vatican Advanced Technology Telescope, and the Boyden 1.52m telescope.

[2]Harvard-Smithsonian Center for Astrophysics, 60 Garden St., Cambridge, MA 02138

[3]NSF Astronomy & Astrophysics Postdoctoral Fellow

[4]Institute of Theoretical Astrophysics, University in Oslo, Norway

[5]Hubble Fellow

[6]Cerro Tololo Inter-American Observatory, National Optical Astronomy Observatory, Casilla 603, La Serena, Chile. NOAO is operated by AURA Inc., under cooperative agreement with the National Science Foundation.

[7]Department of Physics, University of Notre Dame, Notre Dame, IN 46556-5670

[8]Astronomy Department, University of California at Berkeley, Berkeley, CA 94720-3411

[9]University of the Free State, South Africa

revealed a bright fading source (Fox 2002) located at $\alpha_{2000} = 00^h26^m54\overset{s}{.}7$, $\delta_{2000} = +18°55'42''$ (Henden & Levine 2002a). A radio counterpart was found at 22.5 GHz (Frail et al. 2002), 15 GHz (Pooley 2002) and at 86 GHz (Bremer et al. 2002). Polarimetric observations were performed (Covino et al. 2002, Rol et al. 2002). A spectrum showed that the redshift was $z \geq 2.3$ (Chornock & Filipenko 2002), later refined to 2.3351 (Møller et al. 2002). In addition an X-ray afterglow was found (Sako & Harrison 2002).

Several things set this burst apart from other bursts for which afterglows have been observed. Radio observations revealed that the radio afterglow had a very unusual spectrum (Berger, Kulkarni, & Frail 2002). Optical spectra showed several absorption line systems, some being separated from the presumed host galaxy by ~ 3000 km s^{-1} (Chornock & Filippenko 2002, Mirabal et al. 2002, Matheson et al. 2002, Møller et al. 2002). Furthermore, optical spectra showed a significant change in the blue portion of the spectrum whereas the red end did not change (Matheson et al. 2002). In addition to this, the photometric behavior of the optical transient (OT) was highly unusual. The optical afterglow faded quickly, and seemed to exhibit a break (Weidinger et al. 2002) but intensive monitoring revealed that the fading was not as fast as expected (Winn et al. 2002; Halpern et al. 2002a). The afterglow resumed fading (Bersier et al. 2002) but stalled again after ~ 2 days (Stanek et al. 2002). There are also clear deviations from an expected power-law decay, representing variability on short time scales.

Here we report our intensive photometry of the optical transient (OT) during the first night, followed by more occasional monitoring over the next few weeks.

2. Observations

Most of our $UBVR_CI_C$ data were obtained with the F. L. Whipple Observatory (FLWO) 1.2m telescope equipped with the "4Shooter" mosaic camera which delivers a pixel scale of $0\overset{''}{.}335$ per pixel. We continuously monitored the afterglow during the first night, with a typical exposure time of 300 sec. We also obtained several measurements per night for the next five nights. As the burst became fainter, we continued obtaining data (Oct 9 – Oct 12) with the Magellan 6.5m Landon Clay telescope at Las Campanas Observatory, using the Magellan Instant Camera (with a pixel scale is $0\overset{''}{.}069$ per pixel). The typical exposure time for the Magellan observations was 10 minutes in each band.

We also obtained $BVRI$ data during the first night from the CTIO 4m telescope with the MOSAIC II camera. Another early R-band data point comes from the Boyden 1.52m telescope (University of the Free State, South Africa). In addition we observed the optical

transient about 19 days after the burst with the Vatican Advanced Technology Telescope (VATT) 1.8-m telescope.

The data were reduced by several of us using three different photometry packages. We used DoPHOT (Schechter, Mateo & Saha 1993), DAOPHOT II (Stetson, 1987, 1992; Stetson & Harris 1988) and the image subtraction code ISIS (Alard & Lupton 1998, Alard 2000) and we found excellent agreement between the various packages. For consistency, we present the photometry obtained with DAOPHOT throughout this paper. Images were brought onto a common zero point using from 50 to 100 stars per image. We used several stars described by Henden (2002b) to calibrate the instrumental magnitudes, choosing blue stars with colors similar to the OT. In particular, the star located at $\alpha_{2000} = 00^h26^m51\overset{s}{.}4,\ \delta_{2000} = +18°54'36''$ is close to the OT and has very similar colors; it is thus particularly useful for calibrating the photometry.

3. Temporal behavior

It was obvious from early on that the optical afterglow exhibited an unusual behavior. In the first hour after the burst, the OT faded monotonically but this behavior almost stopped after 45 minutes. The OT reached a secondary peak ~ 2.5 hours after the burst. Fading then resumed and the OT more closely followed the usual power law decay now commonly observed in GRBs.

We plot the GRB 021004 $UBVRI$ light curves in the upper panel of Fig.1, omitting the first ~ 10 hours for clarity. Most of the early $UBVRI$ data come from the FLWO 1.2-m telescope (Winn et al. 2002; Bersier et al. 2002; Stanek et al. 2002), with one early R-band point from the Boyden 1.52-m telescope and one $BVRI$ set from the CTIO 4-m telescope, and additional later data ($t > 5.5$ days) from the 6.5-m Magellan and from the 1.8-m VATT telescopes (Garnavich & Quinn 2002). To obtain as clear a picture as possible of the temporal evolution of the afterglow, we also display R-band data taken earlier and in between our data, selecting when possible uniformly reduced data sets as posted on the Gamma-Ray Burst Coordinates Network (GCN; see caption of Fig. 1 for the list of data sets we used). To allow for small differences in the reduction procedures and photometric calibration, uncertainties smaller than 0.05 mag in the GCN data were increased to 0.05 mag. The combined data set has the following number of points: $N(U, B, V, R, I) = (2, 14, 14, 121, 14)$, for a total of 165 points, of which 125 points are our own observations.

To describe the temporal evolution of the GRB 021004 optical counterpart, we fitted the compiled $UBVRI$ data with the smoothly broken power-law model of Beuermann et al.

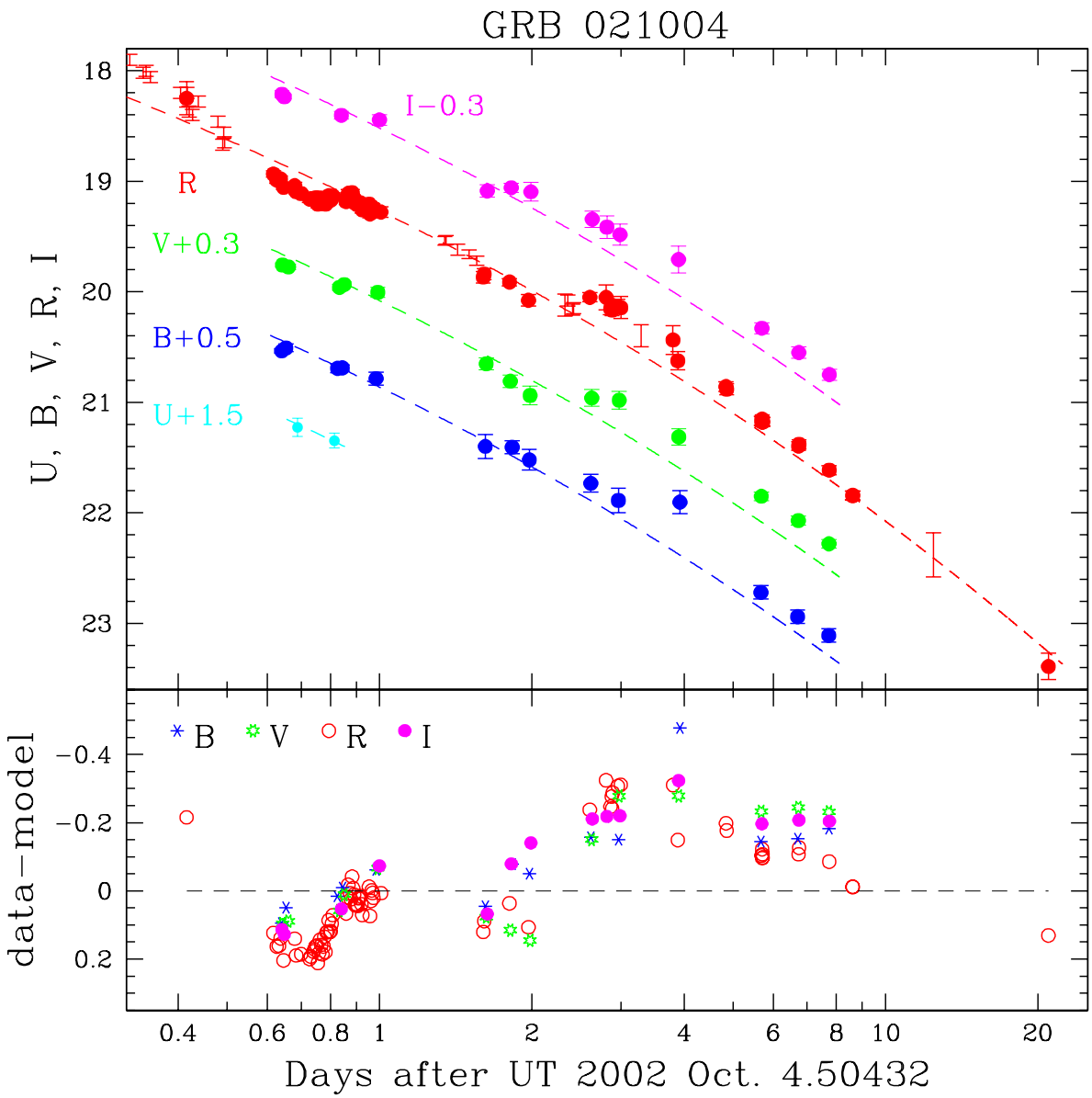

Fig. 1.— *Upper panel: UBVRI* light curves of GRB 021004. Our data are shown with filled circles, data from the GCN are shown with error bars only. We used R-band data from Fox (2002), Uemura et al. (2002), Weidinger et al. (2002), Holland et al. (2002a), Holland et al. (2002b), Sahu et al. (2002), Matsumoto et al. (2002), Masetti et al. (2002), Malesani et al. (2002a), Malesani et al. (2002b), Klotz et al. (2002). Also shown are the simple analytical fits discussed in the text. *Lower panel:* residuals (data−model) for our *BVRI* data. One clearly sees the bumpy character of the light curve as well as the color evolution of the afterglow.

(1999):

$$F_\nu(t) = \frac{2F_{\nu,0}}{\left[\left(\frac{t}{t_b}\right)^{\alpha_1 s} + \left(\frac{t}{t_b}\right)^{\alpha_2 s}\right]^{1/s}} \ , \tag{1}$$

where t_b is the time of the break, $F_{\nu,0}$ is the flux at t_b and s controls the sharpness of the break. This formula describes a power-law $t^{-\alpha_1}$ decline at early times ($t \ll t_b$) and another power-law $t^{-\alpha_2}$ decline at late times (for details see Stanek et al. 2001).

The results of the combined fit are shown as the dashed lines in the upper panel of Fig.1. Clearly, the smooth model is a poor fit to the data but provides a reasonable approximation of the general trend. There are clear "bumps and wiggles" in all bands (except U where we have only two measurements). Due to the poor fit, the parameters obtained would be very different if only a subsample of the data were fitted, or if the data were sampled differently. With these caveats, we report the best-fit values: $\alpha_1 = 0.5, \alpha_2 = 2.4, s \approx 0.3, t_b = 14$ days (we do not give errors on these values). With those parameters the model fits the early (~ 0.01 day) and late R-band data reasonably well.

In the lower panel of Fig.1 we show residuals (data−model) for our $BVRI$ data. Here the bumpy character of the light curve is obvious. What can be also seen is that the broad-band colors of the OT were changing: while VR-bands remained constant to ~ 0.1 mag between the end of night 2 and during night 3 and then decayed by ~ 0.3 mag when observed on night 4, BI-bands decayed by ~ 0.4 mag between the end of night 2 and during night 3, with no further decay in B-band when observed on night 4. In further support of the claim for chromatic decay, it should be mentioned that Rhoads, Burud & Fruchter (2002) reported fading of 0.47 ± 0.04 mag in the H-band between nights 2 and 3, similar to the decay in the I-band over the same time and very different from the behavior in the R-band.

4. Time evolution of the energy distribution

This is the first observed clear example of an OT changing color as it fades. The observed change agrees with the one observed spectroscopically for the same GRB afterglow by Matheson et al. (2002), in the sense that between nights 1 and 3 the afterglow became redder (both $B - V$ and $B - R$ increase). There were spectroscopic observations made on nights beyond night 3 (e.g. Chornock & Filippenko 2002). We predict that they will reveal a reverse change ($B - R$ decreasing when comparing night 4 to night 3) since we see the energy distribution come back to what it was on night 1. We consider the detection of a

significant color changes in the OT of the GRB 021004 to be very secure[10].

The light curves for various colors of the OT are plotted in Fig. 2, in which the color changes are more readily seen. For instance, note the large change in $B-R$ between night 3 and night 4. The OT became bluer, whereas $V-R$ changed only mildly and $R-I$ seems to indicate a redder color. Evidently the shape of the spectral energy distribution (SED) changed significantly $1.5-4$ days after the burst. The Magellan data taken $6-8$ days after the burst indicate that the afterglow has then returned to approximately the same color it had during the first night. We await with interest the results of the final analysis of the multi-band data taken by other observers.

GRB 021004 is located at Galactic coordinates $l = 114\overset{\circ}{.}9187, b = -43\overset{\circ}{.}5615$. To remove the effects of the Galactic interstellar extinction we used the reddening map of Schlegel et al. (1998) which yields $E(B-V) = 0.06$. This corresponds to expected values of Galactic extinction ranging from $A_I = 0.12$ to $A_U = 0.33$.

We synthesized the $UBVRI$ spectrum for the first night and $BVRI$ spectra for later nights from our data by interpolating the magnitudes to a common time for the first night and using our best, most closely-spaced measurements for the other nights (Fig. 3). We converted the magnitudes to fluxes using the effective frequencies and normalizations of Fukugita et al. (1995). These conversions are accurate to about 4%, so to account for the calibration errors we added a 4% error (7% for the U-band) in quadrature to the statistical error in each flux.

There are several important things to notice in Fig. 3. First, the SED on Oct. 5.26 is clearly curved at the blue end. The energy distribution of GRBs is usually a power law in the optical domain (a straight line in Fig. 3; see Garnavich et al. 2002 for a striking example). This is clearly not the case here. Our photometry is in very good agreement with the (independently calibrated) high *Signal/Noise* spectrum also displayed (Matheson et al. 2002). We cannot exclude extra reddening in the host galaxy of the GRB. Another feature, coupled to the color variations discussed above, is the evolution of the shape of the SED, with a most drastic change between UT 7.12 and 8.43. After UT 10.0 the SED comes back to approximately the same shape it had the first night.

The following picture emerges from all of our data: on top of the "normal" decay of the afterglow there seems to be a $30-40\%$ bump, fairly well localized in energy, propagating

[10]To allow the astronomical community to verify our measurements independently, we have placed all of our data, including individual CCD frames, on `anonymous ftp` at `ftp://cfa-ftp.harvard.edu/pub/kstanek/GRB021004`.

from the I-band $1.5 - 2$ days after the burst, through the VR-bands $2.5 - 3$ days after the burst, to the B-band 4 days after the burst. After ~ 6 days the energy distribution comes back to the one it had on the first night. This could be due, as suggested by Rhoads et al. (2002), to "arrival of fresh energy at the blast wave external shock, carried by slow ejecta", but a detailed discussion is beyond the scope of this paper.

5. Short term variations

Encouraged by the detection of short-term variations observed in the optical afterglow of GRB 011211 (Holland et al. 2002c) we decided to spend most of an entire night monitoring this burst in order to search for short term variations. Our data, starting about 14.8 hours after the burst, showed that the fading did indeed continue (Winn et al. 2002). Then, at $\sim$ 18 hours, fading stalled. However, the OT was not constant in brightness during this time. We observed short-term variability on several time scales (see Fig. 4). This has been confirmed independently by Halpern et al. (2002a). We fitted a power law to our first night $UBVRI$ data; this yielded a decay slope of 0.43. A power law is obviously an inadequate description of the OT but it allows us to interpolate the $UBVI$ magnitudes and transform them into an "equivalent" R magnitude[11].

Inspection of Fig. 4 reveals that there is a trend over a few hours (down then up then down again), upon which is superimposed a short term, $\sim 10\%$ variability with a time-scale of 15-30 minutes. This short-term variability is most obvious between 0.75 and 0.8 day, and again between 0.85 and 0.9 day. Such variations might also be present around 0.95 day. We confirmed these variations with three photometry packages. Several nearby comparison stars with brightness comparable to the OT were found to have rms of 0.02-0.025 mag, with no correlated variability present in their light curves. We are therefore confident that the short-term variability is real and is not an artifact of data reduction or statistical fluctuations.

It is only the second time that short-term variations have been observed in a GRB optical afterglow (after GRB 011211: Holland et al. 2002c). Our current data set is much better sampled and allows for better study of this phenomenon. In at least one case, despite very well sampled light curve, no variations larger than ~ 0.02 mag were present (GRB 990510: Stanek et al. 1999). Possible microlensing has been seen in one instance (Garnavich, Loeb & Stanek 2000), however it is probably not the cause of the variations we are seeing here.

[11]The power law index is different from the index α_1 derived in Sect. 3. This is because in this case we fitted our first night data only.

6. Conclusion

Several kinds of models can explain the early ($\sim$ 0.1 day) and later bumps seen on the light curve. For instance Wang & Loeb (2000) showed that density fluctuations in the interstellar medium (ISM) surrounding the GRB can induce significant photometric variability. However other mechanisms might be acting: several models have been proposed specifically for this burst.

Lazzati et al. (2002) consider density fluctuations, either due to a clumpy medium or a wind environment. They favor a clumpy ISM with a density contrast of order 10. Their models reproduce fairly well the first and second bumps in the light curve. They did not try to model later bumps or short-term variability. Nakar, Piran & Granot (2002) considered both a variable density profile (clumpy ISM or stellar wind) and variable energy in the blast wave (refreshed shocks or angular dependence of jet). Both types of models seem to reproduce the R-band light curve fairly well although they do prefer the "patchy shell" model. A possible shortcoming of these models is that the shape of the spectral energy distribution is not supposed to change, whereas we do observe a clear color change. Kobayashi & Zhang (2002) explain the first re-brightening (at $\sim$ 0.1 days) with a reverse shock. However, subsequent to this first bump, their light curve is perfectly smooth they can not explain the later bumps. Other elaborations of this model would have to be included (such as local energy variations or density inhomogeneities).

In conclusion, all models can account reasonably well for the first bump on the light curve but no model yet provides a complete picture of this optical afterglow. Accurate modeling of the later bumps and short term "wiggles" (see Fig. 4) will require more detailed work. Furthermore the changes in the energy distribution will have to be taken into account by future models.

We thank the HETE team, Scott Barthelmy and the GRB Coordinates Network (GCN) for the quick turnaround in providing precise GRB positions to the astronomical community. The amount of data and excitement generated by this unusual burst owe much to the prompt discovery of its optical afterglow and we thank D. Fox for his very early efforts. We thank all the observers who provided their data through the GCN. We thank D. Bennett and K. Cook for help with the Boyden observations. We also thank Jeremy Heyl, Rosalba Perna and Stephen Holland for useful discussions. DB acknowledges support from NSF grant AST-9979812. JNW is supported by an NSF Astronomy & Astrophysics Postdoctoral Fellowship, under grant AST-0104347. PMG acknowledges support from the NASA LTSA grant NAG5-9364. Support for BJM was provided by NASA through a Hubble Fellowship grant from the Space Telescope Science Institute, which is operated by the Association of Universities for

Research in Astronomy, Incorporated, under NASA contract NAS5-26555. DS acknowledges the support of a Smithsonian Astrophysical Observatory Clay Fellowship.

REFERENCES

Alard, C. 2000, A&AS, 144, 363

Alard, C., Lupton, R. H. 1998, ApJ, 503, 325

Berger, E., Kulkarni, S. R., & Frail, D. A. 2002, GCN 1612

Bersier, D., Winn, J., Stanek, K. Z., Garnavich P. M. 2002, GCN 1586

Beuermann, K. et al., 1999, A&A, 352, L26

Bremer, M., et al. 2002, GCN 1590

Chornock, R., & Filippenko, A. V 2002, GCN 1605

Fox, D. W. 2002, GCN 1564

Frail, D. et al. 2002, GCN 1574

Fukugita, M., Shimasaku, K., & Ichikawa, T. 1995, PASP, 107, 945

Garnavich, P. M., Loeb, A., Stanek, K. Z. 2000, ApJ, 544, L11

Garnavich, P., Quinn, J. 2002, GCN 1661

Garnavich, P. M., et al. 2002 ApJ, in press

Halpern, J. P. et al. 2002a, GCN 1578

Henden, A. A., & Levine, S. 2002, GCN 1592

Henden, A. A. 2002, GCN 1630

Holland, S. T. et al. 2002a, GCN 1585

Holland, S. T. et al. 2002b, GCN 1597

Holland, S. T. et al. 2002c, AJ, 124, 639

Kobayashi, S., & Zhang, B. 2002, submitted (astro-ph/0210584)

Klotz, A., Boer, M., & Thuillot, W. 2002, GCN 1615

Landolt, A. 1992, AJ, 104, 340

Lazzati, D., Rossi, E., Covino, S., Ghisellini, G., Malesani, D. 2002, submitted to A&A, (astro-ph/0210333)

Malesani, D. et al. 2002a, GCN 1607

Malesani, D. et al. 2002b, GCN 1645

Masetti, N. et al. 2002, GCN 1603

Matheson, T., P. M. Garnavich, P. M. Foltz, C., West, S., Williams, G., Falco, E., Calkins, M. L., Castander, F. J., Gawiser, E., Jha, S., Bersier, D., & Stanek, K. Z. 2002, submitted to ApJ (astro-ph/0210403)

Matsumoto, K. et al. 2002, GCN 1594

Mirabal, N. et al. 2002a, GCN 1611

Møller, P. et al. 2002, submitted to A&A(astro-ph/0210654)

Nakar, E., Piran, T., Granot, J. 2002 submitted to New Astronomy (astro-ph/0210631)

Pooley, G. 2002, GCN 1588

Sahu, D. K. et al. 2002, GCN 1587

Sako M., & Harrison F. A. 2002, GCN 1624

Schechter, P. L., Mateo, M., Saha, A. 1993, PASP, 105, 1342

Schlegel, D. J., Finkbeiner, D. P., & Davis, M. 1998, ApJ, 500, 525

Shirasaki, Y. et al. 2002, GCN 1565

Stanek, K. Z. et al. 2001, ApJ, 563, 592

Stanek, K. Z., Bersier, D., Winn, J. , Garnavich P. M. 2002, GCN 1598

Stetson, P. B. 1987, PASP, 99 191

Stetson, P. B. 1992, in ASP Conf. Ser. 25, Astrophysical Data Analysis Software and Systems I, ed. D. M. Worrall, C. Bimesderfer, & J. Barnes (San Francisco: ASP), 297

Stetson, P. B., Harris, W. E. 1988, AJ, 96, 909

Uemura, M. et al 2002, GCN 1566

Wang, X. Loeb, A. 2000, ApJ, 535, 788

Weidinger, M. et al. 2002, GCN 1573

Winn, J., Bersier, D., Stanek, K. Z., Garnavich, P. M., Walker, A. 2002 GCN 1576

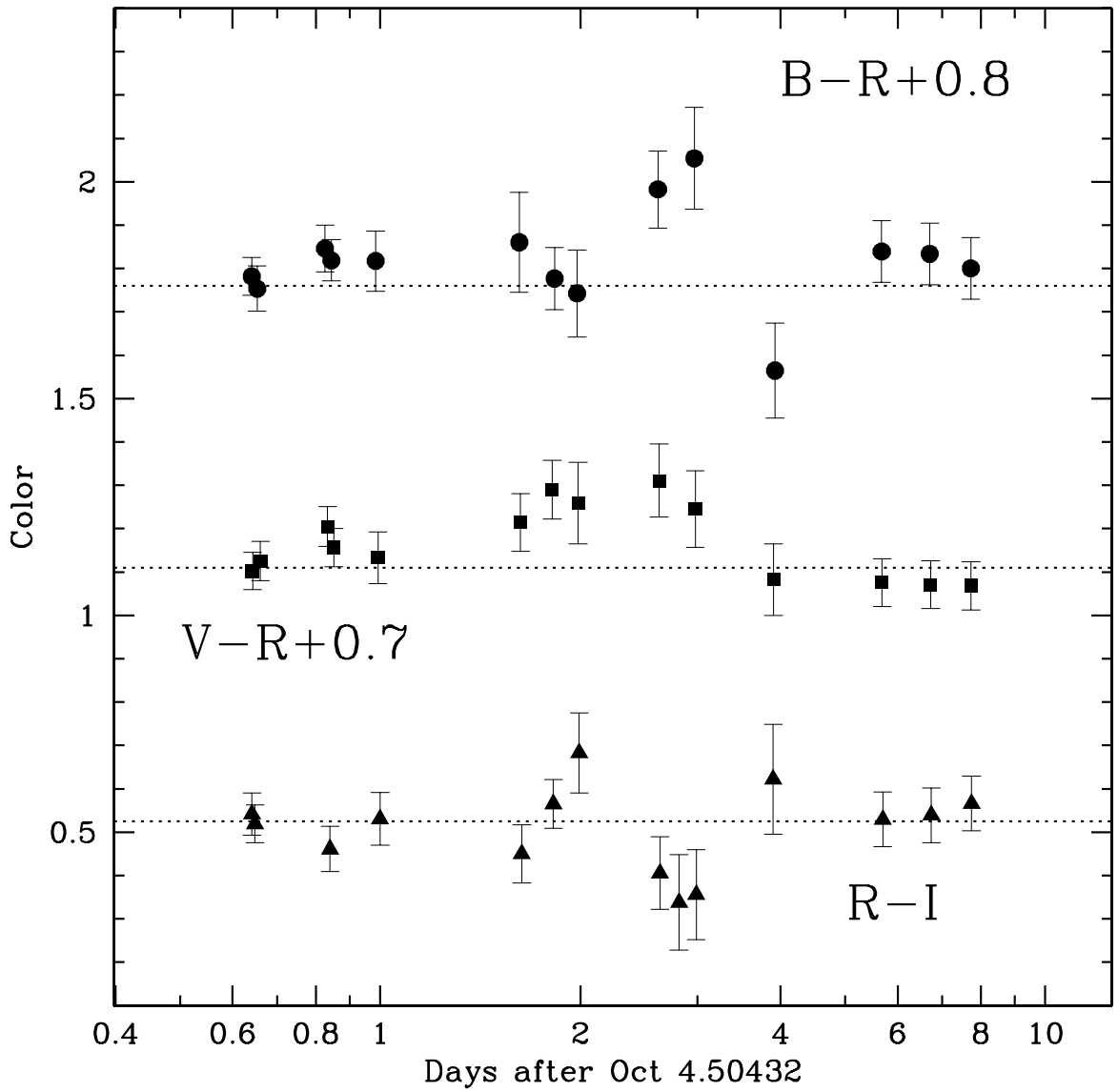

Fig. 2.— Color evolution of the OT in $B-R$ (dots), $V-R$ (squares), and $R-I$ (triangles). The dotted lines are the average color of the first two points.

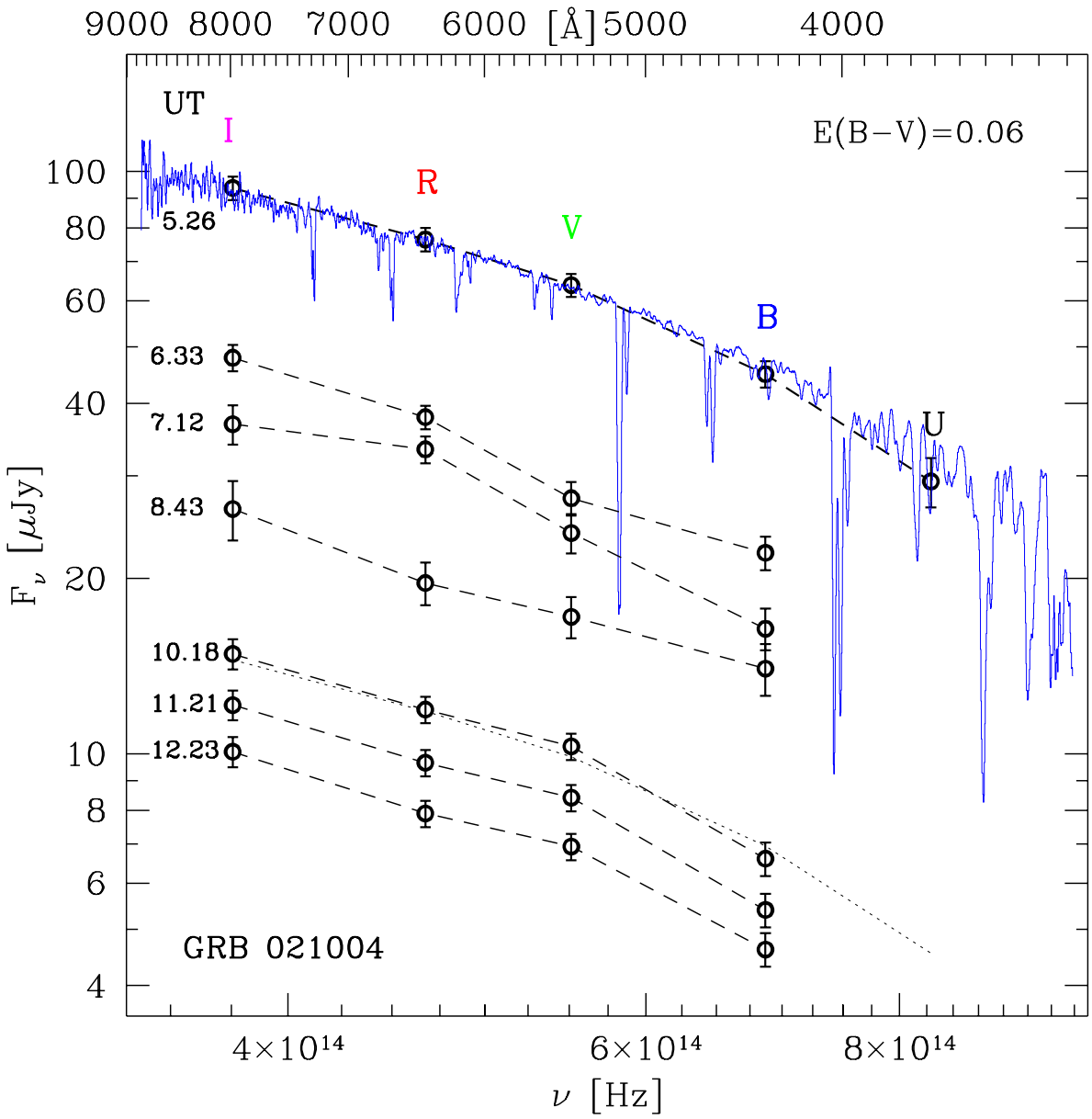

Fig. 3.— Spectral energy distribution (SED) of the optical afterglow of GRB 021004 at various times (indicated on the left side of each SED). We superimposed a spectrum obtained nearly simultaneously with our photometry (Matheson et al. 2002). The SED from UT 5.26 is shown as the dotted line on top of SED from UT 10.18.

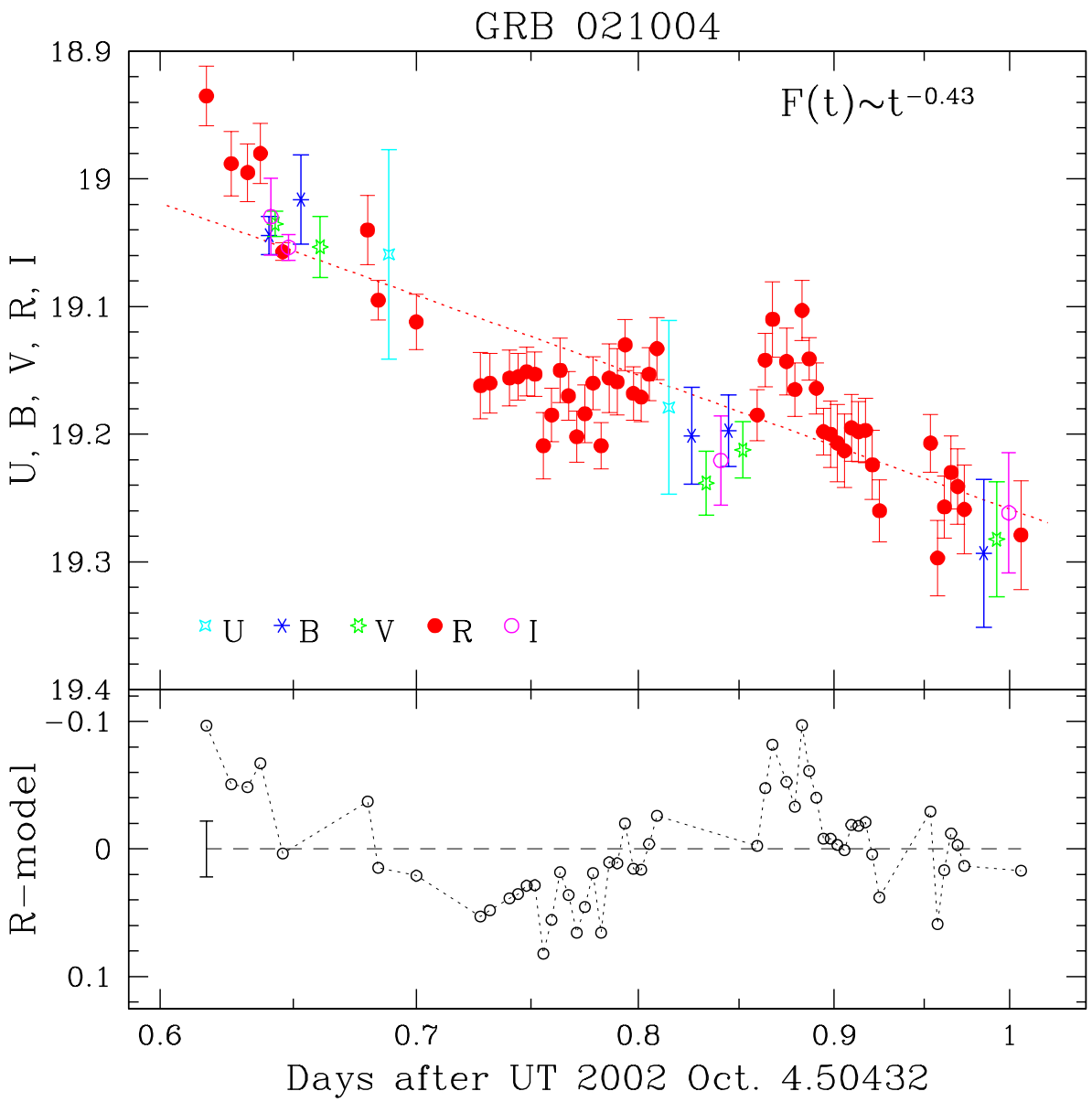

Fig. 4.— *Upper panel* Light curve of the optical afterglow of GRB 021004 during the first night. A power law has been fitted to the data (dotted line). The U, B, V and I data have been shifted (see text for details). *Lower panel* Residuals between this power law model and the data. The error bar on the left is typical for non-variable stars with magnitude similar to the GRB ($rms \sim 0.022$ mag).

Table 1. Photometric data

UT date	m	σ_m	image	filter	t_{exp} (s)	Telescope
5.1929	19.727	0.082	ff1012	U	600.0	FLWO 48”
5.3191	19.847	0.068	ff1037	U	900.0	FLWO 48”
5.1450	20.036	0.020	grb_b2	B	100.0	CTIO 4m
5.1574	20.008	0.035	ff1007	B	600.0	FLWO 48”
5.3304	20.193	0.038	ff1038	B	600.0	FLWO 48”
5.3489	20.189	0.028	ff1041	B	600.0	FLWO 48”
5.4890	20.285	0.058	ff1067	B	600.0	FLWO 48”
6.1226	20.899	0.109	ff1103	B	600.0	FLWO 48”
6.3331	20.907	0.060	ff1109	B	900.0	FLWO 48”
6.4817	21.021	0.093	ff1111	B	600.0	FLWO 48”
7.1203	21.233	0.080	ff1202	B	900.0	FLWO 48”
7.4706	21.388	0.111	ff1212	B	900.0	FLWO 48”
8.4289	21.404	0.103	ff1307	B	1200.0	FLWO 48”
10.1807	22.220	0.060	gg1001	B	600.0	Magellan 6.5m
11.2102	22.440	0.060	gg1101	B	600.0	Magellan 6.5m
12.2311	22.610	0.060	gg1201	B	600.0	Magellan 6.5m
5.1473	19.458	0.020	grb_v2	V	100.0	CTIO 4m
5.1650	19.476	0.024	ff1008	V	600.0	FLWO 48”
5.3377	19.661	0.025	ff1039	V	600.0	FLWO 48”
5.3562	19.635	0.022	ff1042	V	600.0	FLWO 48”
5.4967	19.705	0.045	ff1068	V	600.0	FLWO 48”
6.1299	20.352	0.054	ff1104	V	600.0	FLWO 48”
6.3185	20.509	0.056	ff1107	V	600.0	FLWO 48”
6.4890	20.638	0.086	ff1112	V	600.0	FLWO 48”
7.1311	20.661	0.075	ff1203	V	600.0	FLWO 48”
7.4813	20.682	0.080	ff1213	V	900.0	FLWO 48”
8.4081	21.014	0.073	ff1306	V	1200.0	FLWO 48”
10.1882	21.550	0.040	gg1002	V	600.0	Magellan 6.5m
11.2322	21.770	0.040	gg1102	V	600.0	Magellan 6.5m
12.2385	21.980	0.040	gg1202	V	600.0	Magellan 6.5m
4.9200	18.250	0.150	sa	R	138.0	Boyden 1.52m

Table 1—Continued

UT date	m	σ_m	image	filter	t_{exp} (s)	Telescope
5.1213	18.935	0.027	ff1001	R	300.0	FLWO 48”
5.1306	18.988	0.029	ff1002	R	300.0	FLWO 48”
5.1368	18.995	0.026	ff1003	R	300.0	FLWO 48”
5.1417	18.980	0.027	ff1004	R	300.0	FLWO 48”
5.1503	19.057	0.020	grb_r2	R	100.0	CTIO 4m
5.1841	19.040	0.031	ff1010	R	300.0	FLWO 48”
5.1885	19.095	0.020	ff1011	R	300.0	FLWO 48”
5.2043	19.112	0.025	ff1014	R	300.0	FLWO 48”
5.2319	19.162	0.030	ff1015	R	300.0	FLWO 48”
5.2360	19.160	0.027	ff1016	R	300.0	FLWO 48”
5.2447	19.156	0.025	ff1018	R	300.0	FLWO 48”
5.2485	19.155	0.021	ff1019	R	300.0	FLWO 48”
5.2523	19.151	0.022	ff1020	R	300.0	FLWO 48”
5.2561	19.153	0.020	ff1021	R	300.0	FLWO 48”
5.2599	19.209	0.030	ff1022	R	300.0	FLWO 48”
5.2637	19.185	0.024	ff1023	R	300.0	FLWO 48”
5.2676	19.150	0.029	ff1024	R	300.0	FLWO 48”
5.2714	19.170	0.022	ff1025	R	300.0	FLWO 48”
5.2752	19.202	0.023	ff1026	R	300.0	FLWO 48”
5.2790	19.184	0.026	ff1027	R	300.0	FLWO 48”
5.2828	19.160	0.024	ff1028	R	300.0	FLWO 48”
5.2866	19.209	0.021	ff1029	R	300.0	FLWO 48”
5.2904	19.156	0.031	ff1030	R	300.0	FLWO 48”
5.2942	19.159	0.030	ff1031	R	300.0	FLWO 48”
5.2980	19.130	0.023	ff1032	R	300.0	FLWO 48”
5.3019	19.168	0.024	ff1033	R	300.0	FLWO 48”
5.3057	19.171	0.022	ff1034	R	300.0	FLWO 48”
5.3095	19.153	0.024	ff1035	R	300.0	FLWO 48”
5.3133	19.133	0.028	ff1036	R	300.0	FLWO 48”
5.3636	19.185	0.023	ff1043	R	300.0	FLWO 48”
5.3677	19.142	0.024	ff1044	R	300.0	FLWO 48”

Table 1—Continued

UT date	m	σ_m	image	filter	t_{exp} (s)	Telescope
5.3716	19.110	0.034	ff1045	R	300.0	FLWO 48”
5.3789	19.143	0.030	ff1046	R	300.0	FLWO 48”
5.3833	19.165	0.024	ff1047	R	300.0	FLWO 48”
5.3871	19.103	0.027	ff1048	R	300.0	FLWO 48”
5.3909	19.141	0.019	ff1049	R	300.0	FLWO 48”
5.3947	19.164	0.023	ff1050	R	300.0	FLWO 48”
5.3985	19.198	0.021	ff1051	R	300.0	FLWO 48”
5.4023	19.200	0.030	ff1052	R	300.0	FLWO 48”
5.4061	19.207	0.035	ff1053	R	300.0	FLWO 48”
5.4099	19.213	0.033	ff1054	R	300.0	FLWO 48”
5.4137	19.195	0.030	ff1055	R	300.0	FLWO 48”
5.4176	19.198	0.027	ff1056	R	300.0	FLWO 48”
5.4214	19.197	0.029	ff1057	R	300.0	FLWO 48”
5.4252	19.224	0.031	ff1058	R	300.0	FLWO 48”
5.4292	19.260	0.028	ff1059	R	300.0	FLWO 48”
5.4580	19.207	0.026	ff1060	R	300.0	FLWO 48”
5.4620	19.297	0.034	ff1061	R	300.0	FLWO 48”
5.4660	19.257	0.028	ff1062	R	300.0	FLWO 48”
5.4699	19.230	0.033	ff1063	R	300.0	FLWO 48”
5.4737	19.241	0.034	ff1064	R	300.0	FLWO 48”
5.4775	19.259	0.040	ff1065	R	300.0	FLWO 48”
5.5113	19.279	0.049	ff1070	R	300.0	FLWO 48”
6.1075	19.868	0.053	ff1101	R	600.0	FLWO 48”
6.1150	19.841	0.048	ff1102	R	600.0	FLWO 48”
6.3111	19.913	0.032	ff1106	R	600.0	FLWO 48”
6.4744	20.078	0.052	ff1110	R	600.0	FLWO 48”
7.1090	20.051	0.041	ff1201	R	900.0	FLWO 48”
7.3084	20.051	0.111	ff1205	R	900.0	FLWO 48”
7.3671	20.153	0.054	ff1207	R	600.0	FLWO 48”
7.3806	20.129	0.051	ff1208	R	600.0	FLWO 48”
7.3879	20.167	0.050	ff1209	R	600.0	FLWO 48”

Table 1—Continued

UT date	m	σ_m	image	filter	t_{exp} (s)	Telescope
7.3954	20.124	0.034	ff1210	R	600.0	FLWO 48”
7.4633	20.132	0.063	ff1211	R	600.0	FLWO 48”
7.5029	20.144	0.100	ff1215	R	300.0	FLWO 48”
8.3068	20.436	0.131	ff1302	R	900.0	FLWO 48”
8.3918	20.625	0.082	ff1304	R	600.0	FLWO 48”
9.3453	20.858	0.044	ff1401	R	1200.0	FLWO 48”
9.3596	20.883	0.050	ff1402	R	1200.0	FLWO 48”
10.1960	21.168	0.040	gg1003	R	600.0	Magellan 6.5m
10.2112	21.153	0.040	gg1005	R	300.0	Magellan 6.5m
10.2150	21.180	0.040	gg1006	R	300.0	Magellan 6.5m
10.2187	21.170	0.040	gg1007	R	300.0	Magellan 6.5m
10.2225	21.180	0.040	gg1008	R	300.0	Magellan 6.5m
11.2398	21.396	0.040	gg1103	R	600.0	Magellan 6.5m
11.2560	21.380	0.040	gg1105	R	600.0	Magellan 6.5m
12.2458	21.614	0.040	gg1203	R	600.0	Magellan 6.5m
13.1176	21.842	0.040	gg1301	R	600.0	Magellan 6.5m
13.1249	21.844	0.040	gg1302	R	600.0	Magellan 6.5m
25.5000	23.390	0.120	vatt	R	600.0	VATT 1.8m
5.1457	18.513	0.030	ff1005	I	300.0	FLWO 48”
5.1526	18.537	0.020	grb_i2	I	100.0	CTIO 4m
5.3450	18.704	0.035	ff1040	I	300.0	FLWO 48”
5.5040	18.745	0.047	ff1069	I	600.0	FLWO 48”
6.1372	19.388	0.055	ff1105	I	600.0	FLWO 48”
6.3258	19.359	0.041	ff1108	I	600.0	FLWO 48”
6.4963	19.396	0.084	ff1113	I	600.0	FLWO 48”
7.1384	19.644	0.074	ff1204	I	600.0	FLWO 48”
7.3192	19.715	0.103	ff1206	I	300.0	FLWO 48”
7.4921	19.784	0.096	ff1214	I	900.0	FLWO 48”
8.4042	20.008	0.121	ff1305	I	600.0	FLWO 48”
10.2034	20.630	0.050	gg1004	I	600.0	Magellan 6.5m
11.2470	20.850	0.050	gg1104	I	600.0	Magellan 6.5m

Table 1—Continued

UT date	m	σ_m	image	filter	t_{exp} (s)	Telescope
12.2531	21.050	0.050	gg1204	I	600.0	Magellan 6.5m